attention given to probes and drugs (**Supplementary Table 2**). Currently, more than 800 distinct probes were acquired from six different library sources; while drugs, extracted from five sources (**Supplementary Table 2** and **Supplementary Note 3**), account for more than 11,000 compounds—5,700 of which are annotated as approved drugs. To ensure that various chemical forms (such as stereoisomers or salts) are assigned to only one unique compound, each compound in the P&D portal is converted into its standardized form (**Supplementary Note 2**). However, for cases in which different stereoisomers show different biological impact, original forms still remain available.

To further support the identification of suitable chemical tools, the annotation of P&D compounds is enriched with additional data, such as the bioactivities, targets and pathways in which these compounds take part. These data, obtained from and linked back to various external sources (**Supplementary Table 3**), are organized through ontologies. This ensures consistency between sources and contributes to a high data enrichment. A query can be saved simply by bookmarking its URL, and registered users can create custom compound sets from the arbitrary combination of compounds stored in the P&D library (**Supplementary Note 8**).

The P&D portal is an up-to-date web resource with monthly updates that unifies various commercial and public bioactive compound libraries. Through its flexible and powerful filtering system, it helps users identify high-quality chemical tools for use in chemical biology and drug discovery research.

Data availability statement.

The data on the Probes & Drugs portal are available under the Creative Commons 4.0 license and are available at https://www.probes-drugs.org/data_sources. The code is available at https://www.probes-drugs.org/tools.

Note: Any Supplementary Information and Source Data files are available in the online version of the paper.

ACKNOWLEDGMENTS

We thank J. Baell for editing the PAINS filters and J. Baell and T. Epp for critical reading of the manuscript. This work was supported by the Ministry of Education, Youth and Sports (NPU I–LO1220 to P.B.).

AUTHOR CONTRIBUTIONS

C.S. and P.B. conceived the project; C.S. wrote the software; C.S. and T.M. maintain the database; M.P., J.J., D. Sedlak, M.K. and P.B. curated the data and tested the portal. D. Svozil, C.S., M.K. and P.B. wrote the paper.

COMPETING FINANCIAL INTERESTS

The authors declare no competing financial interests.

Ctibor Skuta[1], Martin Popr[1], Tomas Muller[1], Jindrich Jindrich[1,2], Michal Kahle[1], David Sedlak[1], Daniel Svozil[1,3] & Petr Bartunek[1]

[1]CZ-OPENSCREEN: National Infrastructure for Chemical Biology, Institute of Molecular Genetics AS CR, v. v. i., Prague, Czech Republic. [2]Department of Organic Chemistry, Faculty of Science, Charles University, Prague, Czech Republic. [3]Laboratory of Informatics and Chemistry, Faculty of Chemical Technology, University of Chemistry and Technology Prague, Prague, Czech Republic.
e-mail: bartunek@img.cas.cz

1. Frye, S.V. *Nat. Chem. Biol.* **6**, 159–161 (2010).
2. Bunnage, M.E., Chekler, E.L. & Jones, L.H. *Nat. Chem. Biol.* **9**, 195–199 (2013).
3. Schreiber, S.L. et al. *Cell* **161**, 1252–1265 (2015).
4. Workman, P. & Collins, I. *Chem. Biol.* **17**, 561–577 (2010).
5. Arrowsmith, C.H. *et al. Nat. Chem. Biol.* **11**, 536–541 (2015).
6. Lipinski, C.A. *et al. J. Med. Chem.* **58**, 2068–2076 (2015).

sCMOS noise-correction algorithm for microscopy images

To the Editor: Scientific complementary metal-oxide semiconductor (sCMOS) cameras are rapidly gaining popularity in the biological sciences. The sCMOS sensor provides significant advances in imaging speed, sensitivity and field of view over traditional detectors such as charge-coupled devices (CCD) or electron-multiplying CCDs (EMCCD)[1,2]. However, this sensor introduces pixel-dependent noise; each pixel has its own noise statistics—primarily offset, gain and variance. Left uncorrected, this sCMOS-specific noise generates imaging artifacts and biases in quantification[3]. A suite of algorithms was developed to characterize this noise in each pixel and incorporate the noise statistics in the likelihood function for single-molecule localization[3]. However, these algorithms work exclusively on images with point objects such as in single-particle tracking or single-molecule-switching nanoscopy. No general algorithm that works on conventional microscopy images exists. We developed such an algorithm that dramatically reduces sCMOS noise from microscopy images with arbitrary structures. We show that our new method corrects pixel-dependent noise in fluorescence microscopy using an sCMOS sensor, and this allows the sensor's performance to approach that of an ideal camera.

The fundamental challenge for sCMOS noise correction is the estimation of one of the two variables (with the sum of the variables known); each pixel from an sCMOS camera gives a digital count representing the sum of two variables given by photoelectrons and readout noise, which we consider to follow Poisson and Gaussian distributions, respectively[3]. In the case of detecting point emitters, our extra knowledge is that the photoelectrons form a diffraction-limited spot modeled, for example, as a Gaussian function. Therefore, in spite of the pixel-dependent noise, we demonstrated that the sCMOS-specific maximum-likelihood estimator extracts molecular centers with precision at the theoretical limit[3]. With arbitrary structures, however, the assumption of single emitters is lost.

To develop a generalized noise-correction algorithm, we exploited the common property of microscopy images, the optical transfer function (OTF). The amplitude of the OTF, defined by the microscope's numerical aperture and the wavelength of detection, dictates the frequency-response limit of a microscope system[4,5]. Optical signal from the sample exists only within the frequency limit, while only the contribution from noise lies outside of this limit (**Fig. 1a** and **Supplementary Notes 1–5**). Assuming independent readout noise, we focus on minimizing the noise contribution while maximizing the likelihood of our image estimate to recover the underlying signal buried under the readout noise (**Fig. 1**, **Supplementary Fig. 1** and **Supplementary Notes 6–8**). To this end, we first extract the noise contribution of an image in Fourier space outside or near the theoretical OTF periphery, a conservative estimate of the effective cutoff frequency of a practical system (**Supplementary Note 9**). Then, based on the sCMOS noise model—including the pixel-dependent offset, gain and variance (see **Supplementary Note 10** for sensors with multiple readout units per pixel)—we calculate the likelihood function for the entire image. By minimizing the sum of the noise contribution in Fourier space and the negative log likelihood, we obtain the noise-corrected image (**Fig. 1b** and **Supplementary Fig. 1**). We find that the pixel-dependent noise is, to a large extent, undetectable in the recovered image (**Fig. 1b–e**,

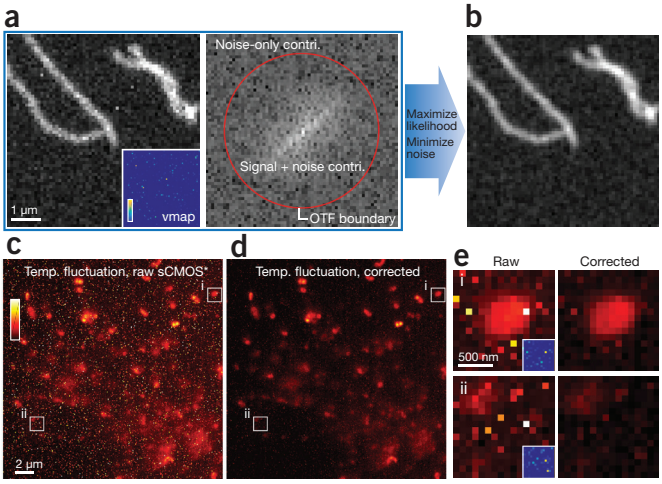

Figure 1 | Concept and results of noise-correction algorithm for sCMOS camera. (**a**) Simulated raw sCMOS image and its components in Fourier space. The inlet image shows the variance map (vmap) of the readout noise. The image in Fourier space consists of contributions (contri.) from both noise and signal. Color map of variance map linearly scales from 2.8 to 2,000 camera count squared (ADU^2). (**b**) The noise-corrected image of the sCMOS image in **a**. (**c**) Temporal (temp.) pixel fluctuation map (s.d. in each pixel over time) over 400 sCMOS frames from experimental data. Color map indicates low (s.d. 1.5 ADU) to high (s.d. 8 ADU) temporal fluctuation per pixel. (**d**) Temporal pixel fluctuation map over 400 noise-corrected images of the sCMOS frames in **c**. (**e**) Zoomed-in images of selected subregions i and ii in **c** and **d**. The inlet images are the variance maps of the corresponding subregions showing the correlation with pixels with high temporal fluctuation in raw sCMOS frames. *, raw sCMOS frames are corrected by sCMOS gain and offset maps to facilitate visual comparison.

Supplementary Figs. 2 and **3**, and **Supplementary Video 1**); and quantification based on the likelihood function shows that the corrected image closely approaches the ideal one (see **Supplementary Note 11** on effects of camera sampling rate). Intensity trace comparisons in fluorescence microscopy images of peroxisome membrane protein and end-binding proteins (EB3) (both tagged with tdEos), and the time series of F-actin tagged with SiR-actin, show a significant reduction of pixel fluctuation while keeping the original signal level intact (**Supplementary Figs. 2** and **3**, **Supplementary Videos 1** and **2** and **Supplementary Methods**). Because our algorithm combines the noise and the likelihood for minimization, it minimizes the noise fluctuation while maintaining the underlying expected photon count and resolution of the image (**Supplementary Figs. 2**, **4**–**6** and **Supplementary Notes 12**–**14**). To demonstrate the correction over the entire field of view, we calculated the temporal fluctuation of individual pixels from a time series. We noticed that the high-readout noise pixels, the hallmark feature of sCMOS images, are absent throughout the entire field of view (**Fig. 1c,d** and **Supplementary Figs. 2**, **3** and **6**).

The developed algorithm (**Supplementary Software** and **Supplementary Note 15**) can generally be applied to sCMOS-based detection and quantitative analysis in a broad spectrum of microscopy techniques—for example, light-sheet microscopy, total internal reflection fluorescence microscopy, fluorescence resonance energy transfer microscopy, speckle microscopy, and conventional fluorescence imaging. The fundamental principle can be applied to other fields where a maximum cutoff frequency exists, such as astronomy and photonics. We hope that these fields can now benefit from the increased quantum efficiency, field of view and imaging speed of sCMOS cameras without compromising its quantitative detection.

Data availability statement.

A sub-stack of unprocessed data used in generating **Supplementary Figure 3** and **Supplementary Video 1** is included in **Supplementary Software**. Additional data that support the findings of this study is available from the corresponding author upon request. The developed software package is available as **Supplementary Software**. Updated versions can be found at https://github.com/HuanglabPurdue/NCS. A **Life Sciences Reporting Summary** for this paper is available.

Note: Any Supplementary Information and Source Data files are available in the online version of the paper.

ACKNOWLEDGMENTS

We thank C. Pellizzari for discussion on algorithm development; D.A. Miller, K.F. Ziegler and P.M. Ivey for helping with the project and for their suggestions on the manuscript. D.M.S. was supported by an NSF grant (1146944-IOS). S.L., M.J.M. and F.H. were supported by grants from the NIH (R35 GM119785) and DARPA (D16AP00093).

AUTHOR CONTRIBUTIONS

S.L., Z.H. and F.H. conceived the project. M.J.M. built the microscope setup. S.L., Z.H. and F.H. developed the algorithm. M.J.M., Y.R., K.M., D.M.S. and F.H. designed the biological imaging samples. S.L. and M.J.M. performed the COS-7 cell experiments. S.L., M.J.M., Y.R. and K.M. performed the neuronal cell experiments. S.L. wrote the software and performed the simulation and analysis. All authors wrote the manuscript.

COMPETING FINANCIAL INTERESTS

The authors declare competing financial interests: details are available in the online version of the paper.

Sheng Liu[1], Michael J Mlodzianoski[1], Zhenhua Hu[2], Yuan Ren[3], Kristi McElmurry[3], Daniel M Suter[3–6] & Fang Huang[1,4,7]

[1]Weldon School of Biomedical Engineering, Purdue University, West Lafayette, Indiana, USA. [2]School of Electrical and Computer Engineering, Purdue University, West Lafayette, Indiana, USA. [3]Department of Biological Sciences, Purdue University, West Lafayette, Indiana, USA. [4]Purdue Institute for Integrative Neuroscience, Purdue University, West Lafayette, Indiana, USA. [5]Bindley Bioscience Center, Purdue University, West Lafayette, Indiana, USA. [6]Birck Nanotechnology Center, Purdue University, West Lafayette, Indiana, USA. [7]Purdue Institute of Inflammation, Immunology and Infectious Disease, Purdue University, West Lafayette, Indiana, USA.
e-mail: fanghuang@purdue.edu

1. von Diezmann, A., Shechtman, Y. & Moerner, W.E. *Chem. Rev.* **117**, 7244–7275 (2017).
2. Huang, Z.-L. *et al. Opt. Express* **19**, 19156–19168 (2011).
3. Huang, F. *et al. Nat. Methods* **10**, 653–658 (2013).
4. Goodman, J.W. *Introduction to Fourier Optics* (Roberts & Company, 2005).
5. Liu, S., Kromann, E.B., Krueger, W.D., Bewersdorf, J. & Lidke, K.A. *Opt. Express* **21**, 29462–29487 (2013).